Acta Pharm. **72** (2022) 79–95
https://doi.org/10.2478/acph-2022-0004

Original research paper

Design, synthesis and molecular modeling study of substituted indoline-2-ones and spiro[indole-heterocycles] with potential activity against Gram-positive bacteria

AWWAD ABDOH RADWAN[1,2,*]
FARES KAED AANAZI[1,3]
MOHAMMED AL-AGAMY[3,4]
GAMAL MOHAMMAD MAHROUS[3]

[1] *Kayyali Chair, College of Pharmacy King Saud University P.O. Box 2457, Riyadh, 11451 Saudi Arabia*

[2] *Department of Pharmaceutical Organic Chemistry, Faculty of Pharmacy Assiut University, Assiut-71527, Egypt*

[3] *Department of Pharmaceutics, College of Pharmacy, King Saud University Riyadh, Saudi Arabia*

[4] *Department of Microbiology and Immunology, Faculty of Pharmacy Al-Azhar University, Cairo, Egypt*

Accepted January 17, 2021
Published online February 12, 2021

Longstanding and firsthand infectious diseases are challenging community health threats. A new series of isatin derivatives bearing β-hydroxy ketone, chalcone, or spiro-heterocycle moiety, was synthesized in a good yield. Chemical structures of the synthesized compounds were elucidated using spectroscopic techniques and elemental analysis. Antibacterial activities of the compounds were then evaluated *in vitro* and by *in silico* modeling. The compounds were more active against Gram-positive bacteria, *Staphylococcus aureus* (*MIC* = 0.026–0.226 mmol L^{-1}) and *Bacillus subtilis* (*MIC* = 0.348–1.723 mmol L^{-1}) than against Gram-negative bacteria (*MIC* = 0.817–7.393 mmol L^{-1}). Only 3-hydroxy-3-(2-(2,5-dimethylthiophen-3-yl)-2-oxoethyl)indolin-2-one (**1b**) was found as active as imipenem against *S. aureus* (*MIC* = 0.026 mmol L^{-1}). *In silico* docking of the compounds in the binding sites of a homology modeled structure of *S. aureus* histidine kinase-Walk allowed us to shed light on the binding mode of these novel inhibitors. The highest antibacterial activity of **1b** is consistent with its highest docking score values against *S. aureus* histidine kinase.

Keywords: 2-indolinone, spiro[indole-heterocyles], antimicrobial, docking study

Pathogenic infectious diseases pose a serious health problem. The mortality rate associated with infectious diseases is rapidly increasing due to a rapid increase in resistance of pathogenic strains (bacteria and fungi) against antimicrobials. This is prompting the search for novel antimicrobial agents to treat new infectious diseases and/or combat existing resistant microbes. Indole scaffold represents an interesting class of biologically active heterocyclic compounds. The scaffold possesses diverse biological activities including anti-inflammatory (1), anticonvulsant (2), antidepressant (3), antiallergic (4), antitubercular (5), antidiabetic (6), antiviral (7) and antimicrobial activity (8–11). Oxindole and other related ring systems also exhibit several biological activities (12–15). Thiosemicarbazone

* Correspondence; e-mail: aradwan@ksu.edu.sa

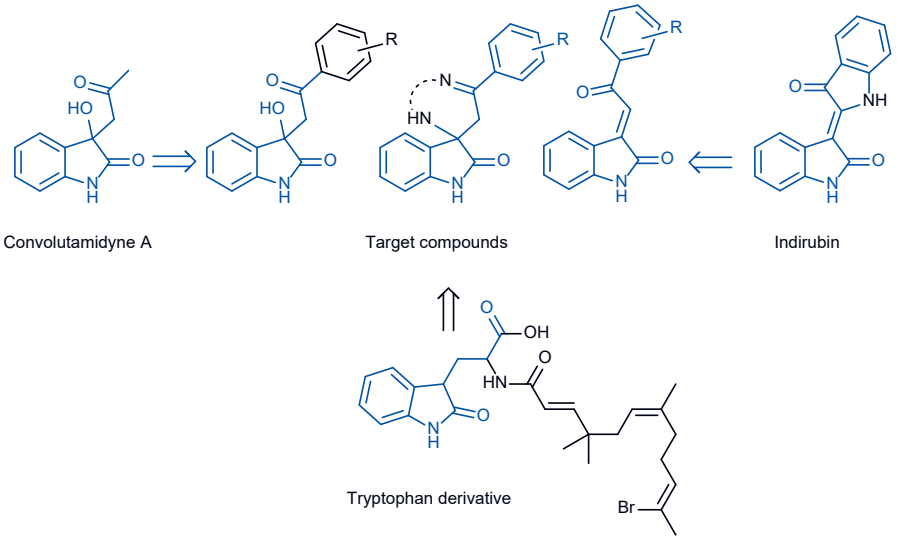

Fig. 1. Representative examples of bioactive heterocyclic molecules with oxindole moiety.

derivatives of indoline-2,3-dione show appreciable antifungal, antibacterial and antiviral activities *in vivo* and *in vitro* (16). New 1,3-dihydro-3-hydroxy-2*H*-indol-2-ones exhibit promising antibacterial and antifungal activities (17, 18). Benzylideneindolone derivatives have potent antimicrobial activity against *Staphylococcus aureus* at μmol L^{-1} concentrations (19).

Furthermore, 1*H*-indole-4,7-diones are potent inhibitors of *Candida krusei*, *Cryptococcus neoformans* and *Aspergillus niger* (20). Indirubin (Fig. 1) is prepared from natural plants (21) and is used in traditional Chinese medicine for the treatment of bacterial and viral infections (22). Further, convolutamydines are representatives of bioactive 3-substituted-3-hydroxy-2-oxindole natural products (Fig. 1) with antioxidant activity (23). In addition, spiroindoline-heterocycles have recently attracted much attention as important antimicrobials (24–26). Tryptophan-linked indole compound (Fig. 1) inhibits the enzymatic activity of histidine kinase (HK) enzyme in an *in vitro* assay (IC_{50} = 43.9 mmol L^{-1}); it also inhibits methicillin-resistant *S. aureus* (MRSA) and vancomycin-resistant *Enterococcus faecalis* (*MIC* = 100 μg mL^{-1} and 50 μg mL^{-1}, resp.) (27).

Bacteria virulence is an adaptive response to extracellular changes through two-component system TCS pathways unique in bacteria (28). The *Staphylococcus aureus* bacteria TCS system comprises HK protein, containing WalK, a membrane-linked sensor protein, and a response regulator protein (RR) containing the DNA-binding domain (WalR) (29). WalK consists of two domains: one domain is a catalytic or ATP-binding domain and the second is a dimerization domain. When HK is activated by external stimuli, ATP binds at the catalytic domain of WalK, and the ATP phosphate group is transferred to a conserved histidine residue on the dimerization domain. Then, the phosphorylation of RR finally results in virulence as one of the bacterial responses to the extracellular stimulus (27). ATP-competitive inhibitors of the microbial HK/WalK are novel antibacterial agents (30, 31).

Given these findings and as a continuation of our work aimed to develop new potential antimicrobial compounds and other bioactive heterocycles based on the oxindole moiety (32–38), we synthesized novel derivatives including spiro[indole-heterocyles] in addition to the indolin-2-one scaffold bearing β-hydroxyl ketone group, chalcone moiety or spiro-heterocycle fragment. We were focused to generate a new lead structure with enhanced antimicrobial activity, possibly inhibiting the histidine kinase activities.

EXPERIMENTAL

Chemistry

Electrothermal IA9300 digital melting point apparatus (Cole-Parmer Ltd., UK) was used to determine the melting points of compounds in sealed tubes. Thin-layer chromatography was used to assess the purity of the compounds on aluminum TLC plates, silica gel coated with fluorescent indicator F254. Perkin Elmer FT-IR system, Spectrum BX (Perkin Elmer, USA) spectrophotometer was used to acquire the IR spectra using KBr-pellet technique, in a region of 4000–400 cm^{-1}. Proton and ^{13}C NMR spectra were recorded by using a 700 MHz spectrometer (Bruker Ascend™ 700, Bruker, USA) in DMSO-d_6 as solvent and TMS as an internal standard. Chemical shifts are shown in δ ppm. Mass spectra were obtained on Agilent 6410B Triple Quadrupole LC/MS spectrometer (Agilent Technologies, USA) using electron spray ionization at ESI 70 eV. Elemental analysis was performed on a 2400 CHNSO Perkin-Elmer analyzer. Chemicals and reagents, used in the study were purchased from Sigma-Aldrich Chemicals, USA).

Syntheses

*General procedure for 3-hydroxy-3-(2-oxo-2-substituted ethyl)-indolin-2-ones (**1a**,**b**).* – A mixture of isatin (1.47 g, 0.01 mol), aryl/heteroaryl methyl ketone (0.01 mol) and diethylamine (1 mL) in ethanol (100 mL) was allowed to stand overnight at room temperature. The yellow needles which formed were recrystallized from ethanol.

*General procedure for 3-(2-oxo-2-substitutedethylidene)indolin-2-ones (**2a**-**c**).* – To a mixture of 0.01 mol of compound **1a** or **1b** in 25 mL abs. ethanol, 50 mL of dilute HCl (25 %) was added. The reaction mixture was allowed to stand overnight and fine orange needles were formed.

*General procedure for spiro-indole-2-one-3,5′-(3-(substituted)-2-pyrazolines) (**3a**-**c**).* – To a mixture of 0.01 mol of respective compound **2** and hydrazine hydrate (50 %) in ethanol (20 mL), diethylamine (1 mL) was added. The reaction mixture was refluxed for 12–14 hours. Glacial acetic acid (10 mL) was added to the cold solution and the obtained precipitate was filtered, washed with ethanol and crystallized from glacial acetic acid.

*General procedure for spiro-indole-2-one-3,6′-(4-(substituted)-5,6-dihydropyrimidine-2-thiones) (**4a**-**f**).* – A mixture of a corresponding compound **2** (0.01 mol), thiourea (0.02 mol), potassium hydroxide (2 g), abs. ethyl alcohol (60 mL) and water (10 mL) was refluxed for 10–12 hours. The reaction mixture was concentrated, cooled and the formed precipitate was filtered, dried, and purified through recrystallization in absolute ethanol.

Table I. Chemical names, molecular formula, elemental analyses, yields and melting points of compounds ***1–4***

Compd.	Chemical name	Molecular formula (M_r)	Yield (%)	M. p. (°C)	CHNS analysis (%) calcd./found
1a	3-Hydroxy-3-(2-(2,5-dichlorophenyl)-2-oxoethyl)-indolin-2-one	$C_{16}H_{11}Cl_2NO_3$ (335.01)	92	183–4	57.16 3.30 4.17 57.01 3.15 3.96
1b	3-Hydroxy-3-(2-(2,5-dimethylthiophen-3-yl)-2-oxoethyl)indolin-2-one	$C_{16}H_{15}NO_3S$ (301.08)	78	199–200	63.77 5.02 4.65 10.64 63.82 4.88 4.57 10.51
2a	3-(2-(2,5-Dichlorophenyl)-2-oxoethylidene) indolin-2-one	$C_{16}H_9Cl_2NO_2$ (317)	80	222–223	60.40 2.85 4.40 60.55 2.71 4.32
2b	3-(2-(Naphthalen-1-yl)-2-oxoethylidene)indolin-2-one	$C_{20}H_{13}NO_2$ (299.09)	72	156–157	80.25 4.38 4.68 80.02 4.45 4.62
2c	3-(2-(2,5-Dimethylthiophen-3-yl)-2-oxoethylidene)indolin-2-one	$C_{16}H_{13}NO_2S$ (283.07)	78	222–223	67.82 4.62 4.94 11.32 68.01 4.54 4.82 11.15
3a	Spiro-indole-2-one-3,5′-(3-(naphthalen-1-yl)-2-pyrazoline)	$C_{20}H_{15}N_3O$ (313.12)	60	203–204	76.66 4.82 13.41 76.71 4.74 13.28
3b	Spiro-indole-2-one-3,5′-(3-(2,5-dimethyl thiophen-3-yl)-2-pyrazoline)	$C_{16}H_{15}N_3OS$ (297.09)	54	182–183	64.62 5.08 14.13 64.53 5.15 14.21
3c	Spiro-indole-2-one-3,5′-(3-(4-methylphenyl) -2-pyrazoline)	$C_{17}H_{15}N_3O$ (277.12)	55	175–176	73.63 5.45 15.15 73.57 5.41 15.26
4a	Spiro-indole-2-one-3,6′-(4-(2,5-dimethoxy-phenyl)-5,6-dihydropyrimidine-2-thione)	$C_{18}H_{15}N_3O_2S$ (337.09)	65	163–164	64.08 4.48 12.45 9.50 63.95 4.42 12.33 9.62
4b	Spiro-indole-2-one-3,6′-(4-(naphthalene-1-yl)-5,6-dihydropyrimidine-2-thione)	$C_{21}H_{15}N_3OS$ (357.09)	60	178–179	70.57 4.23 11.76 8.97 70.41 4.17 11.62 8.86
4c	Spiro-indole-2-one-3,6′-(4-(furan-2-yl)-5,6-dihydropyrimidine-2-thione)	$C_{15}H_{11}N_3O_2S$ (297.06)	52	165–166	60.59 3.73 14.13 10.78 60.51 3.65 13.94 10.69
4d	Spiro-indole-2-one-3,6′-(4-(2,5-dimethylthiophen-3-yl)-5,6-dihydro-pyrimidine-2-thione)	$C_{17}H_{15}N_3OS_2$ (341.07)	54	176–177	59.80 4.43 12.31 18.78 59.72 4.35 12.44 18.86
4e	Spiro-indole-2-one-3,6′-(4-(4-methylphenyl)-5,6-dihydropyrimidine-2-thione)	$C_{18}H_{15}N_3OS$ (321.09)	60	171–172	67.27 4.70 13.07 9.98 67.15 4.78 13.16 9.81
4f	Spiro-indole-2-one-3,6′-(4-(4-methoxyphenyl)-5,6-dihydropyrimidine-2-thione)	$C_{18}H_{15}N_3O_2S$ (337.09)	56	158–159	64.08 4.48 12.45 9.50 64.01 4.35 12.31 9.42

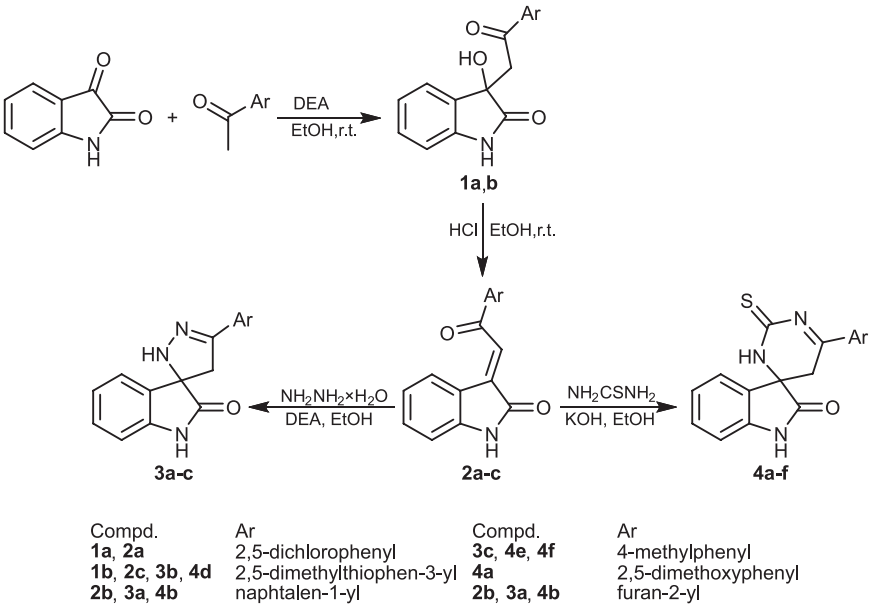

Scheme 1.

Scheme 1 shows the pathway of the synthesis of the target compounds **1a**,**b** to **4a-f**. Their physicochemical data are given in Table I and their chemical structures were elucidated through FT-IR, ^{1}H NMR, ^{13}C NMR and mass spectral data and elemental analyses (Table II).

In vitro *antimicrobial screening*

The activity of compounds (**1a**,**b** to **4a-f**) was evaluated against the Gram-positive bacteria *S. aureus* (ATCC 29213) and *B. subtilis* (ATCC 10400), Gram-negative bacteria *E. coli* (ATCC 35218) and *P. aeruginosa* (ATCC 27853) and fungal strain *C. albicans* (ATCC 2091) which were obtained from the American Type Culture Collection (ATCC, Manassas, VA, USA). Antimicrobial activity was assessed by serial twofold dilution method. Dimethyl sulfoxide (DMSO) was used as a negative control, imipenem was used as a standard drug for antibacterial activity testing and fluconazole was used as a standard drug for antifungal activity testing. All compounds were dissolved in DMSO at the concentration of 2048 μg mL^{-1}. Two-fold dilutions of test and standard compounds were prepared in double strength nutrient broth (bacteria) or Sabouraud dextrose broth (fungi). The stock solutions were serially diluted to give concentrations between 2048 and 8 μg mL^{-1} in the respective nutrient broth. The tubes were inoculated; inoculum size about 10^6 colony forming units (CFU) mL^{-1}. Then, the tubes were incubated at 37 ± 1 °C for 24 h (bacteria) and at 25 °C for 7 days (fungi) and were macroscopically examined for turbidity. The culture tubes showing turbidity (lower concentration) and the culture tube showing no turbidity (higher concentration) gave the minimum inhibitory concentration (*MIC*) of the compound.

Table II. Spectral data of compounds ***1a,b–4a-f***

Compd.	FTIR (λ_{max}, cm^{-1})	^1H NMR (700 MHz, DMSO-d_6, δ ppm)	^{13}C NMR (100 MHz, DMSO-d_6, δ ppm)	MS (*m*/*z*): [M^+] calcd./found
1a	3456–3346 (O-H, N-H), 3150 (ArC-H), 2962 (AliphC-H), 1700 (C=O), 1623 (C=O)	3.51, 3.88 (1H, 1H, d, non-equivalent CH_2), 6.18 (1H, s, OH), 6.81–7.58 (ArH, m, 7H), 10.34 (1H, s, NH)	49.98 (CH_2), 73.59 (indole C3), 110.02 (indole-CH), 121.78(indole-CH), 124.61(indole-CH), 128.82(indole-CH), 129.26 (indole-CH), 129.70(Ph-CH), 131.37(Ph-CH), 132.42(Ph-C), 132.53(Ph-C), 132.59(Ph-CH), 139.89(Ph-C), 143.04 (indole-arC, 178.25 (C=O indole), 198.11 (C=O oxoethyl)	335.01 335.0
1b	3410–3363 (O-H, N-H), 3126 (Ar-CH), 1708 (C=O), 1656 (C=O)	2.38 (3H, s, CH_3), 2.41 (3H, s, CH_3), 3.41 and 3.81 (2H, d, non-equivalent CH_2), 6.00 (1H, s, OH), 6.80–7.27 (ArH, m, 5H), 10.23 (1H, s, NH)	15.05 (CH_3), 15.91 (CH_3), 49.18 (CH_2), 73.31 (indole-C3), 119.80 (indole-CH), 121.54 (indole-CH), 124.08 (indole-CH), 127.09 (indole-C), 129.31 (indole-CH), 132.27 (thiophene-CH), 135.40 (thiophene-C), 135.57 (thiophene-C), 143.42 (indole-C), 146.59 (thiophene-C), 178.81 (indole-CO), 192.76 (oxoethyl-CO)	301.08 301.01
2a	3250 (NH), 3198 (Ar-CH), 1700 (C=O), 1623 (C=O)	6.81–7.86 (ArH, m, 7H), 8.28 (CO-CH=C<), 10.34 (1H, s, NH)	110.02 (indole-CH), 121.77 (indole-C), 124.60 (indole-CH), 127.98 (indole-CH), 128.81 (indole-CH), 129.69 (oxoethyl-C1), 130.04 (Ph-CH), 131.36 (Ph-CH), 132.42 (Ph-C), 132.53 (Ph-C), 132.58 (Ph-CH), 139.89 (Ph-C), 143.04 (indole-C), 146.09 (indole-C3), 178.25 (indole-CO), 198.11 (oxyethyl-CO)	317.00 316.89
2b	3211 (NH), 3063 (Ar-CH), 1705 (C=O), 1622 (C=O)	6.91–8.24 (ArH, m, 11H), 8.74 (CO-CH=C<, s, 1H), 10.86 (1H, s, NH)	110.89 (napth-CH), 120.46 (indole-CH), 122.25 (indole-C), 125.51 (indole-CH), 125.63 (indole-CH), 127.21 (indole-CH), 127.26 (naph-CH), 128.94 (naph-CH), 129.25 (naph-CH), 129.30 (naph-CH), 130.07 (naph-CH), 130.88 (naph-C), 134.04 (naph-CH), 134.41 (naph-CH), 134.96 (naph-C), 136.38 (indole-C), 145.45 (indole-C3), 168.77 (indol-CO), 194.67 (oxyethyl-CO)	299.09 299.02
2c	3221 (NH), 3190 (Ar-CH), 1707 (C=O), 1640 (C=O)	2.4 (3H, s, CH_3), 2.69 (3H, s, CH_3), 6.87–7.57 (ArH, m, 5H), 8.8 (CO-CH=C<), 10.77 (1H, s, NH)	14.96 (CH_3), 16.25 (CH_3), 110.75 (indole-CH), 120.48 (thiophene-C4), 122.30 (indole-CH), 126.85 (indole-CH), 127.26 (thiophene-CH), 128.76 (oxoethyl-C1), 133.18 (thiophene-C5), 135.8 (indole-CH), 136.24 (indole-CH), 136.88 (thiophene-C3), 145.18 (indole-C), 146.56 (indole-C3), 148.88 (thiophene-C2), 168.88, 186.86	283.07 283.01
3a	3361 (NH), 3138 (Ar-CH), 1681 (C=O)	3.57, 3.64 (2H, d, non-equivalent CH_2), 6.82–8.00 (11H, m, ArH), 10.56 (2H, s, NH)	46.61 (pyrazoline-C4), 56.51 (pyrazoline-C5), 110.21 (indole-CH), 121.65 (indole-CH), 122.72 (indole-CH), 124.85 (naph-CH), 125.82 (naph-CH), 126.08 (naph-CH), 126.42 (naph-CH), 127.35 (indole-CH), 127.59 (indole-CH), 127.78 (naph-C), 127.90 (indole-C), 133.99 (indole-C), 148.42 (pyrazoline-C3), 176.84 (indole-CO)	313.12 313.05

Compd.	FTIR (λ_{max}, cm^{-1})	^1H NMR (700 MHz, DMSO-d_6, δ ppm)	^{13}C NMR (100 MHz, DMSO-d_6, δ ppm)	MS (m/z): [M^+] calcd./found
3b	3356 (NH), 3154 (Ar-CH), 1680 (C=O)	2.36 (3H, s, CH_3), 2.52 (3H, s, CH_3), 3.29, 3.40 (2H, d, non-equivalent CH_2), 6.83–7.68 (5H, m, ArH), 10.36 (2H, s, two NH)	15.02 (CH_3), 15.04 (CH_3), 46.48 (pyrazoline-C4), 69.14 (pyrazoline-C5), 110.08 (indole-CH), 122.62 (indole-CH), 124.03 (indole-CH), 125.36 (indole-CH), 129.53 (thiophene-CH), 129.89 (thiophene-C), 131.98 (thiophene-C), 134.56 (thiophene-C), 135.22 (indole-C), 141.87 (indole-C), 145.63 (pyrazoline-C3), 178.79 (indole-CO)	297.09 297.01
3c	3295, 3150, 1680 (C=O)	2.32 (3H, s, CH_3), 3.29, 3.44 (non-equivalent 1H, 1H, s, CH_2), 6.85–8.45 (8H, m, ArH), 10.42 (1H, s, NH), 11.10 (1H, s, NH)	21.38 (CH_3), 44.25 (pyrazoline-C4), 69.58 (pyrazoline-C5), 110.13 (indole-CH), 121.64 (indole-CH), 122.71 (indole-CH), 124.26 (indole-CH), 126.19, 129.77 (Ph-CH), 132.81 (Ph-CH), 141.92 (indole-C), 147.92 (indole-C), 156.12 (pyrazoline-C3), 179.17 (indole-CO)	277.12 277.03
4a	3315 (NH), 1695 (CS), 1615 (CO)	3.38 (3H, s, CH_3O), 3.50, 3.78 (1H, 1H, d, non-equivalent CH_2), 3.67 (3H, s, OCH_3), 6.67–7.17 (7H, m, ArH), 9.61 (2H, s, NH)	32.02 (pyrimidinethione-C5), 52.61 (CH_3O), 55.57 (CH_3O), 55.88 (pyrimidinethione-C6), 112.50 (Ph-CH), 114.55 (Ph-CH), 115.63 (Ph-CH), 116.32 (Ph-CH), 117.98 (indole-CH), 120.40 (indole-CH), 126.12 (indole-CH), 128.63 (indole-CH), 132.58 (indole-C), 134.25 (indole-C), 150.52 (Ph-C), 153.40 (Ph-C), 162.79 (pyrimidinethione-C4), 172.62 (C=O), 186.02 (C=S)	367.10 366.94
4b	3219 (NH), 1690 (CS), 1617 (CO)	3.66, 3.68 (1H, 1H, d, non-equivalent CH_2), 6.93–8.15 (11H, m, ArH), 9.34 (1H, s, NH), 10.85 (1H, s, NH)	30.52 (pyrimidinethione-C5), 52.43 (pyrimidinethione-C6), 124.01 (indole-CH), 125.30 (indole-CH), 125.95 (indole-CH), 126.85 (naph-CH), 127.43 (naph-CH), 128.38 (naph-CH), 128.74 (naph-CH), 128.98 (naph-CH), 129.70 (naph-CH), 130.09 (naph-CH), 130.87 (indole-CH), 133.30 (naph-C), 133.98 (naph-C), 135.33 (naph-C), 135.69 (indole-C), 154.29 (indole-C), 164.19 (pyrimidinethione-C4), 183.61 (CO), 202.22 (CS)	357.09 356.95
4c	3367 (NH), 1701 (CS), 1617 (CO)	3.61 (2H, s, CH_2), 6.43–7.92 (7H, m, ArH), 9.72 (1H, s, NH), 10.72 (1H, s, NH)	40.87 (pyrimidinethione-C5), 52.49 (pyrimidinethione-C6), 112.25 (furan-C3), 113.37 (furan-C4), 114.77 (indole-CH), 123.37 (indole-CH), 126.21 (indole-CH), 130.63 (indole-CH), 132.93 (indole-C), 137.94 (indole-C), 141.56 (furan-C2), 145.01 (furan-C5), 154.59 (pyrimidinethione-C3), 163.97 (CO), 183.90 (CS)	297.06 296.93
4d	3315 (NH), 1695 (CS), 1615 (CO)	2.42 (3H, s, CH_3), 2.58 (3H, s, CH_3), 3.37, 3.64 (1H, 1H, d, non-equivalent CH_2), 6.12–7.57 (5H, m, ArH), 9.43 (1H, s, two NH), 10.23 (1H, s, NH)	13.81 (CH_3), 15.96 (CH_3), 30.32 (pyrimidinethione-C5), 52.45 (pyrimidinethione-C6), 114.28 (thiophene-C4), 116.55 (thiophene-C3), 125.07 (indole-CH), 127.04 (indole-CH), 128.68 (indole-CH), 132.87 (indole-CH), 134.46 (thiophene-C5), 135.27 (thiophene-C2), 137.10 (indole-C), 146.02 (indole-C), 163.90 (pyrimidinethione-C3), 172.49 (CO), 185,27 (CS)	341.07 340.93

Compd.	FTIR (λ_{max}, cm^{-1})	^{1}H NMR (700 MHz, DMSO-d_6, δ ppm)	^{13}C NMR (100 MHz, DMSO-d_6, δ ppm)	MS (*m/z*): [M$^+$] calcd./found
4e	3447 (NH), 1700 (CS), 1654 (CO)	2.73 (3H, s, CH_3), 3.66, 3.68 (non-equivalent 1H, 1H, d, CH_2), 6.00–8.02 (8H, m, ArH), 10.10 (2H, s, two NH)	21.53 (CH_3), 30.52 (pyrimidinethione-C5), 52.44 (pyrimidinethione-C6), 125.17 (indole-CH), 125.35 (indole-CH), 125.53 (indole-CH), 126.96 (indole-CH), 128.36 (Ph-CH), 128.57 (Ph-CH), 129.04 (Ph-C), 130.08 (Ph-C), 133.33 (indole-C), 136.88 (indole-C), 164.17 (pyrimidinethione-C3), 172.51 (CO), 183.61 (CS)	321.09 320.89
4f	3400 (NH), 1724 (CS), 1618 (CO)	3.67 (3H, s, CH_3O), 3.77, 3.87 (non-equivalent 1H, 1H, d, CH_2), 6.66–8.07 (8H, m, ArH), 9.57 (1H, s, NH), 10.79 (1H, s, NH)	40.88 (CH_3O), 52.44 (pyrimidinethione-C5), 55.65 (pyrimidinethione-C6), 113.98 (Ph-CH), 124.37 (indole-CH), 130.67 (indole-CH), 130.76 (indole-CH), 131.42 (indole-CH), 131.64 (Ph-C), 132.28 (Ph-CH), 137.10 (indole-C), 137.60 (indole-C), 154.60 (Ph-C), 160.10 (pyrimidinethione-C3), 163.68 (CO), 183.55 (CS)	337.09 337.01

Molecular modeling

Homology modeling. – The sequence of histidine kinase subunit A (Q7A2R7, 471 residues) (39) of *S. aureus* (strain Mu50/ATCC 700699) was used as a query for BLAST sequence-database search to identify similar X-ray structures (40). The structures were then ranked based on similarity percent. The top-ranked PDB entry was selected as a template for the alignment with Q7A2R7 and homology model building using the Modeller program (41). During modeling, the original position of the adenosine-5′-[beta,gamma--methylene]triphosphate (ACP ligand), as the X-ray ligand bound to the protein structure of the 5c93.pdb in the crystal structure, was retained to rebuild the binding cavity. The model of histidine kinase subunit A generated by homology modeling was used for the preparation of the input receptor files in the Dock6.4 program (42). The structures of the newly synthesized active compounds were used for flexible docking inside the binding site of the model using default dock6 parameters and Grid score including van der Waals and electrostatic target-ligand interaction of the ligand--binding conformation and the internal energy.

Docking study. – Molecular docking study was performed by using the Dock6.4 program on Ubuntu 14.2 (desktop Linux operating system) supported Dell 5000 Laptop, Processor, Intel(R) Core(TM) i7-5500U CPU @ 2.40GHz and system type 64-bit operating system, x64-based processor. Chemical structures of compounds **1a,b** to **4a-f** were generated in the protonated state under physiological conditions. The model of histidine kinase subunit A was used in the docking process without further minimization. Using the default settings of the program and defining a sphere of 10 Å diameter around the center of the binding pocket, the co-crystallized ligand was docked in the original protein structure. The resulting solutions were clustered based on the heavy atom root-mean-square deviation (RMSD) values (two superimposed atomic coordinates represent two different conformations only when RMSD > 1 Å). During docking, all torsion angles of the compound were set to free rotation and 10 binding poses per ligand were obtained. The binding pose with the highest total score was taken into consideration for ligand-receptor interactions.

RESULTS AND DISCUSSION

Chemistry

Scheme 1 shows the synthesis pathway of compounds **1a**,**b** to **4a-f**. Compounds 2,3-hydroxy-3-(2-oxo-2-substituted ethyl)-indolin-2-ones (**1a**,**b**) were obtained through the condensation of isatin with the appropriate acetophenone in the presence of diethylamine. In ethanolic HCl, compounds **1** underwent dehydration resulting in 3-(2-oxo-2-substituted ethylidene)indoline-2-ones (**2a-c**). The reaction of compounds **2a-c** with hydrazine hydrate led to hydrazone formation with subsequent intra-cyclization through nucleophilic Michael addition reaction resulting in spiro[indole-pyrazoline] compounds **3a-c**. The reaction of compounds **2a-c** with thiourea resulted in the formation of spiro[indole-dihydropyrimidine] compounds **4a-f**.

The compounds' structure was established based on IR, ^{1}H NMR, ^{13}C NMR and mass spectral, and elemental analysis data. IR spectra of **1a**,**b** revealed two characteristic bands at 1708–1700 cm^{-1} and 1656–1623 cm^{-1} (two C=O groups) and one band at 3456–3346 cm^{-1} (OH). The latter band disappeared upon conversion of compounds **1a**,**b** into compounds **2a-c** which showed only two characteristic bands at 1707–1700 cm^{-1} and 1640–1622 cm^{-1} (two C=O groups). On the other hand, compounds **3a-c** showed characteristic bands at 1800 cm^{-1} (one C=O group) while compounds **4a-f** showed characteristic bands at 1724–1695 cm^{-1} (C=S group) and at 1654–1615 cm^{-1} (one C=O group).

^{1}H NMR spectra of compounds **1a**,**b** were characterized by the appearance of both OH signals at δ 5.83–6.18 ppm and non-equivalent methylene protons signals at δ 3.32-3.73 and δ 3.67–4.07 ppm. These signals disappeared, with the concomitant appearance of a singlet at δ 8.1–8.34 ppm associated with -CO-CH=C< moiety, in compounds **2a-c** confirming their formation. ^{1}H NMR spectra of compounds **3a-c** and **4a-f** were characterized by the appearance of non-equivalent methylene protons signals at δ 3.25–3.79 and δ 3.35–3.83 ppm, and at δ 3.37–3.66 and δ 3.64–3.78 ppm, resp. ^{13}C NMR spectra of compounds **1a**,**b** revealed characteristic signals at δ 49.8–49.18 ppm (CH_2 group), δ 73.59–73.31 ppm (indole-C3) and δ 198.11–192.76 ppm (oxoethyl-CO). Compounds **2a-c** showed characteristic signals at δ 146.56–145.45 ppm (indole-C3) and δ 198.11–186.86 ppm (oxoethyl-CO). On the other hand, ^{13}C NMR spectra of compounds **3a-c** showed characteristic signals at δ 46.61–44.25 (pyrazoline-C4) and at δ 69.58–56.51 (pyrazoline-C5) while compounds **4a-f** showed characteristic signals at δ 52.44–30.02 ppm (pyrimidinethione-C5) and at δ 55.88–52.43 (pyrimidinethione-C6).

Elemental analyses of the synthesized compounds **1a**,**b**–**4a-f** revealed that the mass percentage values found for carbon, hydrogen, nitrogen and sulfur were in accordance with the calculated values. The spiro compounds **3a-c** and **4a-f** showed higher nitrogen percentage values (> 11 %) than the compounds **1a**,**b** and **2a-c** (nitrogen percentage values > 5 %).

Antimicrobial screening

Table III shows the results of antimicrobial screening of compounds **1a**,**b**–**4a-f**. The compounds showed weak antifungal activity, however, marked antibacterial activity was obtained. Compounds **1a**,**b** to **4a-f** showed promising activity against Gram-positive

Table III. Minimum inhibitory concentrations (MIC) of compounds ***1a,b–4a-f***

Compd.	*MIC* (mmol L^{-1})				
	Gram-positive bacteria		Gram-negative bacteria		Fungus
	B. subtilis	*S. aureus*	*E. coli*	*P. aeuroginosa*	*C. albicans*
1a	0.382	0.047	> 6.11	> 6.11	> 6.11
1b	0.425	0.026	0.85	1.7	3.4
2a	1.615	0.05	> 6.46	> 6.46	> 6.46
2b	0.856	0.107	6.849	> 6.849	> 6.849
2c	1.809	0.226	3.618	1.809	3.618
3a	0.817	0.102	0.817	1.635	3.271
3b	0.43	0.053	1.723	> 6.895	> 6.895
3c	0.924	0.057	3.696	> 7.393	> 7.393
4a	0.348	0.087	1.395	> 5.58	> 5.58
4b	1.434	0.044	2.868	> 5.736	> 5.736
4c	1.723	0.053	1.723	> 6.895	> 6.895
4d	0.75	0.046	1.501	> 6.005	> 6.005
4e	0.797	0.049	3.19	> 6.38	> 6.38
4f	0.379	0.047	3.038	> 6.077	> 6.077
Imipenem	0.026	0.026	0.026	0.026	–
Fluconazole	–	–	–	–	0.0008

bacteria with the higher activity against *S. aureus* (*MIC* = 0.026–0.226 mmol L^{-1}) than *B. subtilis* (*MIC* = 0.348–1.723 mmol L^{-1}) and fair activity against Gram-negative bacteria (*MIC* = 0.817 – 7.393 mmol L^{-1}). As far as *S. aureus* is concerned compounds **1a**,**b** (*MIC* = 0.026–0.047 mmol L^{-1}) are more active than compounds **2a-c** (*MIC* = 0.05–0.226 mmol L^{-1}) and **3a-c** and **4a-f** (*MIC* 0.044–0.102 mmol L^{-1}).

Acid-catalysed dehydration of β-hydroxy ketone, compound **1a** (*MIC, S. aureus,* 0.047 mmol L^{-1}) resulted in almost as active chalcone compound **2a** (*MIC, S. aureus,* 0.05 mmol L^{-1}). Moreover, β-hydroxy ketone **1b** was found equipotent with the reference drug imipenem (*MIC, S. aureus,* 0.026 mmol L^{-1}), however, transforming it into chalcone type candidate produced a nine-fold less potent compound **2c** (*MIC, S. aureus,* 0.226 mmol L^{-1}). Transformation of the chalcone **2b** (*MIC, S. aureus* 0.107 mmol L^{-1}) into spiro[indole-pyrazoline] led to compound **3a** with comparable antibacterial activity (*MIC, S. aureus* 0.102 mmol L^{-1}), however, its cyclization into spiro[indole-dihydropyrimidinethione] produced compound **4b** with 2.5-fold enhanced potency (*MIC, S. aureus* 0.044 mmol L^{-1}). Cyclization of the least active compound **2c** produced active spiro[indole-pyrazoline] **3b** (*MIC, S. aureus* 0.053 mmol L^{-1}), and spiro[indole-dihydropyrimidinethione] **4d** (*MIC, S. aureus* 0.046 mmol L^{-1}).

Molecular modeling study

The 3D structure of *S. aureus* histidine kinase is unavailable. Therefore, to investigate the possible interactions between compounds **1a**,**b** to **4a**-**f** and the amino acids that form the binding site of *S. aureus* histidine kinase, homology modeling of the sequence entry Q7A2R7 with subsequent docking process were performed. Using the BLAST alignment protocol, the crystal structure of a monomer histidine kinase domain complex with ACP (5c93.A) of *E. coli* (43), was chosen as a template. The choice was based on BLAST-p alignment and top pairwise percentage residue identity (36.53 %) and similarity (38 %). During homology modeling, after the heavy atoms have been modeled and all hydrogen atoms added, the protein coordinates were minimized using the AMBER94 force field. Briefly, the structure is a compact single domain with 5-stranded β-sheet and 7-α-helices and random coils (Fig. 2). The

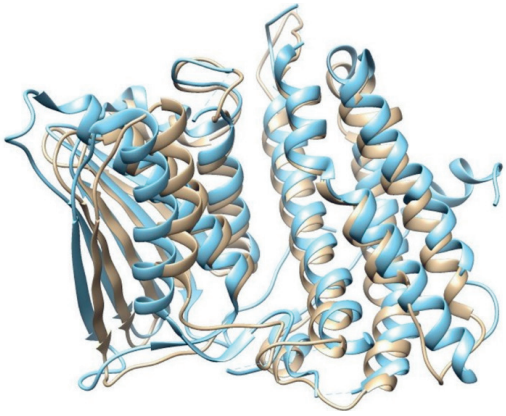

Fig. 2. The backbone structure of *S. aureus* histidine kinase (Q7A2R7) (homolog model, colored cyan) overlayed onto that of 5c93A.pdb (template structure, colored grey).

Table IV. Results of docking study of compounds ***1a,b–4a-f***

Compd.	Amino acid(s) of the receptor involved in the H-bond	H-bond distance (Å)	Grid score energy (kcal mol^{-1})	Es energy (kcal mol^{-1})	VDW energy (kcal mol^{-1})
1a	Gly 418	2.293	–34.250	–1.030	–33.220
	Leu 421	2.093			
1b	Gly 418	2.148	–36.231	–0.697	–35.534
2a	Gly 420	2.439	–30.423	–0.407	–30.016
2b	Gly 418	2.569	–30.165	0.686	–30.851
2c	Tyr 362	2.369	–33.296	0.413	–33.709
	Lys 361	2.361			
3a	Leu 421	2.125	–31.692	0.313	–32.005
3b	Leu 421	1.809	–31.698	0.524	–32.222
3c	Asn 358	1.975	–29.757	–0.026	–29.731
4a	Asn 358	2.286	–22.402	0.242	–22.644
	Leu 419	2.477			
4b	Asn 417	2.079	–23.424	1.551	–24.975
4c	Asn 358	2.364	–19.967	–1.588	–18.379
	Asn 417	1.746			
4d	Lys 361	1.825	–23.323	–1.006	–22.327
4e	Lys 361	2.051	–20.883	–1.422	–22.305
	Asn 358	2.162			
4f	Lys 361	2.247	–23.597	–0.578	–23.019

Es – electrostatic energy, VDW energy – van der Waals energy

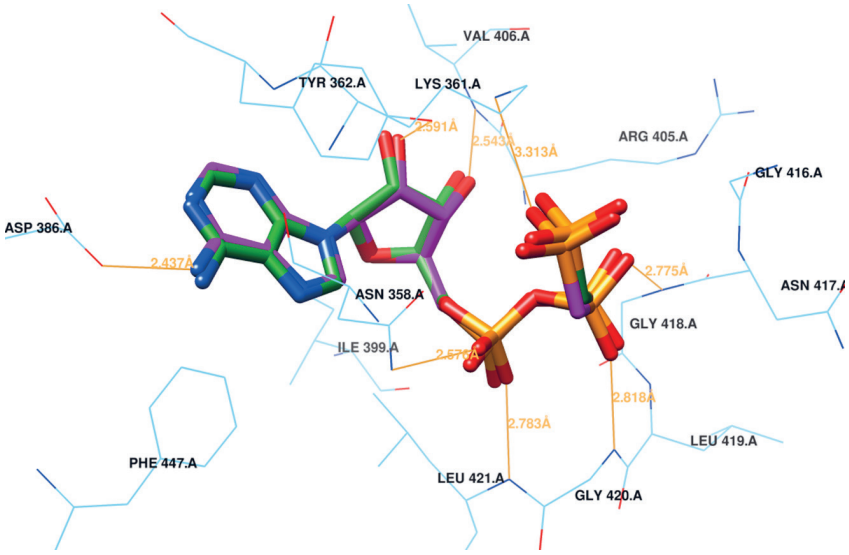

Fig. 3. The co-crystallized ACP (from 5c93.pdb, colored magenta) and the re-docked ACP structure (colored forest green), superimposed inside the binding site of homology-modeled Q7A2R7.

RMSD value of the pose from the redocking of the ACP structure itself (0.704 Å) confirmed the appropriateness of the docking approach (Fig. 3). The binding site includes a hydrophobic pocket delineated with the side-chains of Asp 358, Lys 361, Tyr 362, Asp 386, Ile 399, Arg 405, Val 406, Gly 416, Asn 417, Gly 418, Leu 419, Gly 420, and Leu 421.

The docking poses of the newly synthesized compounds **1a,b** to **4a-f** showed hydrogen bonding between the C-3 hydroxyl group of the isatin moiety, the C-2 carbonyl oxygen of the isatin moiety, the carbonyl oxygen of the acetophenone moiety and the NH group of the binding site residues Asn 417, Asn 418 Gly 420, Asn 358, Tyr 360 or Asn 461 (Fig. 4 and Table IV). The derived docking scores for compounds **1a,b** to **4a-f** were in agreement with

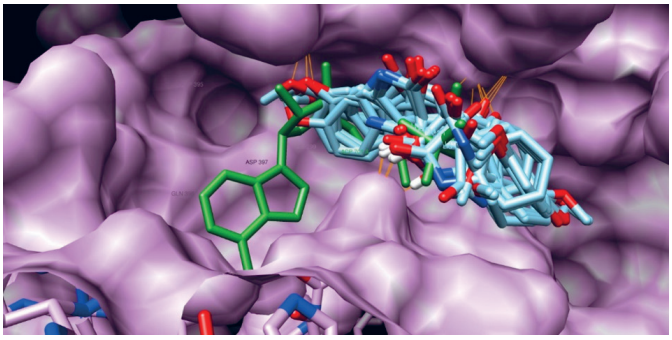

Fig. 4. The newly synthesized compounds (colored cyan) overlaid the X-ray ligand ACP (colored forest green) inside the binding site, hydrogen bonds are displayed in orange color).

the obtained *MIC*s against *S. aureus* and also with the notion that the antibacterial effects of indoline-2-one derivatives might be associated with the inhibition of the histidine kinase-mediated pathway (44). 3-Hydroxy-3-(2-(2,5-dimethylthiophen-3-yl)-2-oxoethyl) indolin-2-one (compound 1b) was found most active against *S. aureus* (*MIC* = 0.026 mmol L^{-1}) and also showed the top-score in the docking study (grid score in energy –36.231 kcal mol^{-1}) (Tables III and Table IV).

CONCLUSIONS

In summary, a series of new isatin compounds bearing either β-hydroxyketone or chalcone moieties were synthesized and biologically evaluated for their antimicrobial activity. The compounds showed promising activity against Gram-positive bacteria with the highest specific activity against *S. aureus.* 3-Hydroxy-3-(2-(2,5-dimethylthiophen-3-yl)-2-oxoethyl)indolin-2-one (**1b**) was the most active against *S. aureus* (*MIC* 0.026 mmol L^{-1}) equivalent to the value exerted by imipenem, whereas compounds **1a**, **2a**, **3b**,**c** and **4b-f** showed comparable activity (*MIC* = 0.044–0.057 mmol L^{-1}). The highest activity of **1b** against *S. aureus* is consistent with its highest docking score values inside the binding site of *S. aureus* histidine kinase (grid score –36.231 kcal mol^{-1}, electrostatic energy –0.697 kcal mol^{-1}, and van der Waals energy –35.534 kcal mol^{-1}). The main contribution to the docking grid score is from van der Waals energy that reflects high geometric complementarity which is well known essential for the specific binding.

Analysis of the binding mode of compounds **1a**,**b** to **4a-f** to a modeled-structure of histidine kinase revealed that these compounds had the same orientation in the binding site, and the same hydrogen bonding as well as the X-ray ligand ACP. The high activity of compounds **1a**,**b** are supposed to be attributed to the free rotation of the isatin scaffold around the bond between indole-C3 and methylene group of the oxyethyl substituent. This flexibility plays role in binding efficiency with the histidine kinase receptor. The higher activity and top-ranked docking score of compound **1b** suggest it as a lead compound for further optimization to design and synthesize more potent and selective anti-*S. aureus* compounds.

Acknowledgments. – The authors would like to extend their sincere appreciation to the Deanship of Scientific Research at King Saud University for funding this research group (no. RG 1435-080).

Supplementary material is available upon request.

REFERENCES

1. S. K. Sridhar and A. Ramesh, Synthesis and pharmacological activities of hydrazones, Schiff and Mannich bases of isatin derivatives, *Biol. Pharm. Bull.* **24** (2001) 1149–1152; https://doi.org/10.1248/bpb.24.1149
2. M. Verma, S. N. Pandeya, K. N. Singh and J. P. Stables, Anticonvulsant activity of Schiff bases of isatin derivatives, *Acta Pharm.* **59** (2004) 49–56.
3. A. K. Ádám, S. Grzegorz, J. B. Andrzej and M. K. György, Spiro[pyrrolidine-3,3′-oxindoles] and their indoline analogs as new 5-HT6 receptor chemotypes, *Molecules* **22** (2017) Article ID 2221; https://doi.org/10.3390/molecules22122221

4. E. Siddalingamurthy, K. M. Mahadevan, N. M. Jagadeesh and M. N. Kumara, Synthesis and docking study of 3-(*N*-alkyl/aryl piperidyl) indoles with serotonin-5HT, H1 and CCR2 antagonist receptors, *Int. J. Pharm. Pharm. Sci.* **6** (2014) 475–482.
5. N. Karal, A. Gursoy, F. Kandemirli, N. Shvets, F. B. Kaynak, S. Ozbey, V. Kovalishyn and A. Dimoglo, Synthesis and structure-antituberculosis activity relationship of 1*H*-indole-2,3-dione derivatives, *Bioorg. Med. Chem.* **15** (2007) 5888–5904; https://doi.org/10.1016/j.bmc.2007.05.063
6. Q. Xu, L. Huang, J. Liu, L. Ma, T. Chen, J. Chen, F. Peng, D. Cao, Z. Yang, N. Qiu, J. Qiu, G. Wang, X. Liang, A. Peng, M. Xiang, Y. Wei and L. Chen, Design, synthesis and biological evaluation of thiazole- and indole-based derivatives for the treatment of type II diabetes, *Eur. J. Med. Chem.* **52** (2012) 70–81; https://doi.org/10.1016/j.ejmech.2012.03.006
7. A. I. Hashem, A. S. Youssef, K. A. Kandeel and W. S. Abou-Elmagd, Conversion of some 2(3*H*)-furanones bearing a pyrazolyl group into other heterocyclic systems with a study of their antiviral activity, *Eur. J. Med. Chem.* **42** (2007) 934–939; https://doi.org/10.1016/j.ejmech.2006.12.032
8. P. Kumar, S. Singh and M. R. F. Pratama, Synthesis of some novel 1*H*-indole derivatives with antibacterial activity and antifungal activity, *Lett. App. NanoBioSci*. **9** (2020) 961–967; https://doi.org/10.33263/LIANBS92.961967
9. R. V. Singh, N. Fahmi and M. K. Biyala, Coordination behavior and biopotency of N and S/O donor ligands with their palladium(II) and platinum(II) complexes, *J. Iranian Chem. Soc*. **40** (2005) 40–46; https://doi.org/https://doi.org/10.1007/BF03245778
10. K. Meenakshi, G. Sammaiah, M. Sarangapani and R. J. Venkateswar, Synthesis and antimicrobial activity of 1-*N*-piperidinomethyl isatin-3-[N-(quinolin-8-yloxy) acetyl] hydrazones, *Indian J. Heterocycl. Chem.* **16** (2006) 21–24.
11. W. Hong, J. Li, Z. Chang, X. Tan, H. Yang, Y. Ouyang, Y. Yang, S. Kaur, I. C. Paterson, Y. F. Ngeow and H. Wang, Synthesis and biological evaluation of indole core-based derivatives with potent antibacterial activity against resistant bacterial pathogens, *J. Antibiot.* **70** (2017) 832–844; https://doi.org/10.1038/ja.2017.55
12. M. Taha, E A. J. Aldhamin, N. B. Almandil, El H. Anouar, N. Uddin, M. Alomari, F. Rahim, B. Adalat, M. Ibrahim, F. Nawaz, N. Iqbal, B. Alghanem, A. Altolayyan and K. M. Khan, Synthesis of indole based acetohydrazide analogs: Their *in vitro* and *in silico* thymidine phosphorylase studies, *Bioorg. Chem.* **98** (2020) Article ID 103745; https://doi.org/10.1016/j.bioorg.2020.103745
13. T. Tokunaga, H. W. Ewan, T. Umezome, K. Okazaki, Y. Ueki, K. Kumagai, S. Hourai, J. Nagamine, H. Seki, M. Taiji, H. Noguchi and R. Nagata, Oxindole derivatives as orally active potent growth hormone secretagogues, *J. Med. Chem.* **44** (2001) 4641–4649; https://doi.org/10.1021/jm0103763
14. T. Tokunaga, H. W. Ewan, J. Nagamine and R. Nagata, Structure-activity relationships of the oxindole growth hormone secretagogues, *Bioorg. Med. Chem. Lett.* **15** (2005) 1789–1792; https://doi.org/10.1016/j.bmcl.2005.02.042
15. P. E. Romo, B. Insuasty, R. Abonia, M. del Pilar Crespo and J. Quiroga, Synthesis of new oxindoles and determination of their antibacterial properties, *Heteroatom Chem.* **2020** (2020) Article ID 8021920 (9 pages); https://doi.org/10.1155/2020/8021920
16. K. N. Aneesrahman, K. Ramaiah, G. Rohini, G. P. Stefy, N. S. P. Bhuvanesh and A. Sreekanth, Synthesis and characterisations of copper(II) complexes of 5-methoxyisatin thiosemicarbazones: Effect of N-terminal substitution on DNA/protein binding and biological activities, *Inorg. Chim. Acta* **492** (2019) 131–141; https://doi.org/10.1016/j.ica.2019.04.019
17. A. A. El-Gendy and A. M. Ahmed, Synthesis and antimicrobial activity of some new 2-indolinone derived oximes and spiro-isoxazolines, *Arch. Pharm. Res.* **23** (2000) 310–314; https://doi.org/10.1007/bf02975439
18. A. L. Davis, D. R. Smith and T. J. McCord, Synthesis and microbiological properties of 3-amino-1-hydroxy-2-indolinone and related compounds, *J. Med. Chem.* **16** (1973) 1043–1045; https://doi.org/10.1021/jm00267a020

19. O. Sureyya and O. Z. Semiha, A Study of 3-substituted benzylidene-1,3-dihydro-indoline derivatives as antimicrobial and antiviral agents, *Z. Naturforsch. C* **64c** (2009) 155–162; https://doi.org/10.1515/znc-2009-3-401
20. C. K. Ryu, J. Y. Lee, R. E. Park, M. Y. Ma and J. H. Nho, Synthesis and antifungal activity of 1H-indole-4,7-diones, *Bioorg. Med. Chem. Lett.* **17** (2007) 127–131; https://doi.org/10.1016/j.bmcl.2006.09.076
21. R. Hoessel, S. Leclerc, J. A. Endicott, M. E. Nobel, A. Lawrie, P. Tunnah, M. Leost, E. Damiens, D. Marie, D. Marko, E. Niederberger, W. Tang, G. Eisenbrand and L. Meijer, Indirubin, the active constituent of a Chinese antileukaemia medicine, inhibits cyclin-dependent kinases, *Nat. Cell Biol.* **60** (1999) 60–67; https://doi.org/10.1038/9035
22. R. Han, Highlight on the studies of anticancer drugs derived from plants in China, *Stem Cells* **12** (1994) 53–63; https://doi.org/10.1002/stem.5530120110
23. H. P. Zhang, Y. Kamano, Y. Ichihara, H. Kizu, K. Komiyama, H. ltokawa and G. R. Pettit, Isolation and structure of convolutamydines B – D from marine bryozoan Amathia convolute, *Tetrahedron* **51** (1995) 5523–5528; https://doi.org/10.1016/0040-4020(95)00241-Y
24. A. Abdel-Rahman, E. Keshk, M. Hanna and S. El-Bady, Synthesis and evaluation of some new spiro indoline-based heterocycles as potentially active antimicrobial agents, *Bioorg. Med. Chem.* **12** (2004) 2483–2488; https://doi.org/10.1016/j.bmc.2003.10.063
25. S. Rajeev, S. P. Siva, K. Leena, K. Shilpi and C. J. Subhash, Design and synthesis of spiro[indole-thiazolidine]spiro[indole-pyrans] as antimicrobial agents, *Bioorg. Med. Chem. Lett.* **21** (2011) 5465–5469; https://doi.org/10.1016/j.bmcl.2011.06.121
26. P. Maryam, A. Sakineh, and M. Mojtaba, Synthesis and antibacterial evaluation of novel spiro[indole-pyrimidine]ones, *J. Heterocycl. Chem.* **55** (2018) 173–180; https://doi.org/10.1002/jhet.3021
27. T. Kitayama, R. Iwabuchi, S. Minagawa, S. Sawada, R. Okumura, K. Hoshino, J. Cappiello and R. Utsumi, Synthesis of a novel inhibitor against MRSA and VRE: preparation from zerumbone ring opening material showing histidine-kinase inhibition, *Bioorg. Med. Chem. Lett.* **17** (2007) 1098–1101; https://doi.org/10.1016/j.bmcl.2006.11.015
28. A. M. Stock, V. L. Robinson and P. N. Goudreau, Two-component signal transduction, *Annu. Rev. Biochem.* **69** (2000) 183–215; https://doi.org/10.1146/annurev.biochem.69.1.183
29. R. Gao, and A. M. Stock, Biological insights from structures of two-component proteins, *Annu. Rev. Microbiol.* **63** (2009) 133–154; https://doi.org/10.1146/annurev.micro.091208.073214
30. K. E. Wilke and E. E. Carlson, All signals lost, *Sci. Transl. Med.* **5** (2013) Article ID 203ps12; https://doi.org/10.1126/scitranslmed.3006670
31. A. E. Bem, N. Velikova, M. T. Pellicer, P. V. Baarlen, A. Marina and J. M. Wells, Bacterial histidine kinases as novel antibacterial drug targets, *ACS Chem Biol.* **10** (2015) 213–224; https://doi.org/10.1021/cb5007135
32. A. A. Radwan and W. Abdel-Mageed, *In silico* studies of quinoxaline-2-carboxamide 1,4-di-n-oxide derivatives as antimycobacterial agents, *Molecules* **19** (2014) 2247–2260; https://doi.org/10.3390/molecules19022247
33. A. A. Radwan, F. K. Alanazi and M. H. Al-Agami, 1,3,4-Thiadiazole and 1,2,4-triazole-3(4*H*)-thione bearing salicylate moiety: synthesis and evaluation as anti-*Candida albicans*, *Braz. J. Pharm. Sci.* **53** (2017) e15239; https://doi.org/10.1590/s2175-97902017000115239
34. T. Abul-Fadl, A. A. Radwan, H. A. Abdel-Aziz, B. Mohamed, I. A. Mohamad, K. Adnan, Novel Schiff bases of indoline-2,3-dione and nalidixic acid hydrazide: synthesis, *in vitro* antimycobacterial and *in silico Mycobacterium tuberculosis* (mtb) DNA gyrase inhibitory activity, *Dig. J. Nanomater. Bios.* **7** (2012) 329–336.
35. T. Aboul-Fadl, A. A. Radwan, M. I. Attia, A. Al-Dhfyan and H. A. Abdel-Aziz, Schiff bases of indoline-2,3-dione (isatin) with potential antiproliferative activity, *Chem. Cent. J.* **6** (2012) Article ID 49; https://doi.org/10.1186/1752-153X-6-49

36. A. A. Radwan, Structure-based virtual screening for novel EGFR kinase inhibitors using the zinc database, *Lat. Am. J. Pharm.* **34** (2015) 1107–1112.

37. A. A. Radwan, F. Al-Mohanna, F. K. Alanazi, P. S. Manogaran and A. Al-Dhfyan, *Bioorg. Med. Chem. Lett.* **26** (2016) 1664–1670; https://doi.org/10.1016/j.bmcl.2016.02.064

38. A. A. Radwan and F. K. Alanazi, *In silico* studies on novel inhibitors of MERS-CoV: Structure-based pharmacophore modeling, database screening and molecular docking, *Trop. J. Pharm. Res.* **17** (2018) 513–517; https://doi.org/http://dx.doi.org/10.4314/tjpr.v17i3.18

39. M. Kuroda, T. Ohta, I. Uchiyama, T. Baba, H. Yuzawa, I. Kobayashi, L. Cui, A. Oguchi, K. Aoki, Y. Nagai, J.-Q. Lian, T. Ito, M. Kanamori, H. Matsumaru, A. Maruyama, H. Murakami, A. Hosoyama, Y. Mizutani-Ui and K. Hiramatsu, Whole genome sequencing of methicillin resistant *Staphylococcus aureus*, *Lancet* 357 (2001) 1225–1240; https://doi.org/10.1016/S0140-6736(00)04403-2

40. C. Camacho, G. Coulouris, V. Avagyan, N. Ma, J. Papadopoulos, K. Bealer and T. L. Madden, BLAST+: architecture and applications, *BMC Bioinform.* **10** (2009) 421–430; https://doi.org/10.1186/1471-2105-10-421

41. F. András and A. Sali, Modeller: generation and refinement of homology-based protein structure models, *Meth. Enzymol.* **374** (2003) 461–491; https://doi.org/10.1016/S0076-6879(03)74020-8

42. P. T. Lang, S. R. Brozell, S. Mukherjee, E. F. Pettersen, E. C. Meng, V. Thomas, R. C. Rizzo, D. A. Case, T. L. James and I. D. Kuntz, DOCK 6: combining techniques to model RNA-small molecule complexes, *RNA* **15** (2009) 1219–1230; https://doi.org/10.1261/rna.1563609

43. Y. Cai, M. Su, A. Ahmad, X. Hu, J. Sang, L. Kong, X. Chen, C. Wang, J. Shuai and A. Han, Conformational dynamics of the essential sensor histidine kinase WalK, *Acta Crystallogr. D* **73** (2017) 793–803; https://doi.org/10.1107/S2059798317013043

44. E. Geisinger, E. A. George, J. Chen, T. W. Muir and R. P. Novick, Identification of ligand specificity determinants in AgrC, the Staphylococcus aureus quorum-sensing receptor, *J. Biol. Chem.* **283** (2008) 8930–8938; https://doi.org/10.1074/jbc.M710227200